0090-9556/02/3012-1512–1522$7.00
DRUG METABOLISM AND DISPOSITION
DMD 30:1512–1522, 2002

Vol. 30, No. 12
789/1027900
Printed in U.S.A.

QUINIDINE AND HALOPERIDOL AS MODIFIERS OF CYP3A4 ACTIVITY: MULTISITE KINETIC MODEL APPROACH

ALEKSANDRA GALETIN, STEPHEN E. CLARKE, AND J. BRIAN HOUSTON

School of Pharmacy and Pharmaceutical Sciences, University of Manchester, Manchester, United Kingdom (A.G., J.B.H.); and Department of Mechanism and Extrapolation Technologies, GlaxoSmithKline, Welwyn, Hertfordshire, United Kingdom (S.E.C.)

(Received May 9, 2002; accepted September 9, 2002)

This article is available online at http://dmd.aspetjournals.org

ABSTRACT:

The selection of appropriate substrates for investigating the potential inhibition of CYP3A4 is critical as the magnitude of effect is often substrate-dependent, and a weak correlation is often observed among different CYP3A4 substrates. This feature has been attributed to the existence of multiple binding sites and, therefore, relatively complex in vitro data modeling is required to avoid erroneous evaluation and to allow prediction of drug-drug interactions. This study, performed in lymphoblast-expressed CYP3A4 with oxidoreductase, provides a systematic comparison of the effects of quinidine (QUI) and haloperidol (HAL) as modifiers of CYP3A4 activity using a selection of CYP3A4 substrates: testosterone (TST), midazolam (MDZ), nifedipine (NIF), felodipine (FEL), and simvastatin (SV). The effect of QUI and HAL on CYP3A4-mediated pathways was substrate-dependent, ranging from potent inhibition of NIF (K_i = 0.25 and 5.3 μM for HAL and QUI, respectively), weak inhibition (TST), minimal effect (HAL on MDZ/SV) to QUI activation of FEL and SV metabolism. Inhibition of TST metabolite formation occurred but its autoactivation properties were maintained, indicating binding of a QUI/HAL molecule to a distinct effector site. Various multisite kinetic models have been applied to elucidate the mechanism of the drug-drug interactions observed. Kinetic models with two substrate-binding sites have been found to be appropriate to a number of interactions, provided the substrates show hyperbolic (MDZ, FEL, and SV) or substrate inhibition kinetic properties (NIF). In contrast, a three-site model approach is required for TST, a substrate showing positive cooperativity in its binding to CYP3A4.

To assess the in vivo significance of drug-drug interactions involving P450[1] inhibition from in vitro data, it is necessary to identify the particular P450 enzymes involved, estimate their contribution to the overall elimination of the drug, and characterize the inhibition effects (Ito et al., 1998; Rodrigues et al., 2001; Tucker et al., 2001). The latter is the most problematic factor, because it is dependent on the appropriate selection of both an inhibition model to derive a K_i value and an inhibitor concentration at the enzyme active site.

The selection of an appropriate inhibition model for CYP3A4 is particularly difficult because this enzyme frequently does not obey Michaelis-Menten kinetics, shows substrate-dependent effects (Kenworthy et al., 1999; Stresser et al., 2000; Wang et al., 2000; Lu et al., 2001), and is prone to activation (Shou et al., 1994; Tang et al., 1999; Kenworthy et al., 2001) in addition to inhibition effects in drug-drug interaction studies. Substrate auto- and heteroactivation (Shou et al., 1999; Domanski et al., 2000; Ngui et al., 2000; Kenworthy et al., 2001), partial inhibition (Wang et al., 1997, 2000), substrate inhibition (Lin et al., 2001; Schrag and Wienkers, 2001), and pathway differential kinetics (Shou et al., 2001a) observed for CYP3A4 are attributed to the different binding domains for the substrate and modifier within the enzyme active site. Involvement of multiple binding sites may result in an inhibition effect at only one site or a differential effect at each site, confounding a straightforward prediction of a potential in vivo interaction. A description of the molecular events, incorporating the binding of multiple substrate/inhibitor molecules, requires relatively complex modeling.

To provide a mechanistic insight for atypical enzyme properties shown by CYP3A4, various approaches have been reported in recent years (Hosea et al., 2000; Tang and Stearns, 2001), involving either the simultaneous binding of two molecules (Korzekwa et al., 1998; Shou et al., 2001b) or the existence of a separate effector-binding site (Ueng et al., 1997; Kenworthy et al., 2001). Additional evidence for the existence of multiple binding sites is provided by site-directed mutagenesis studies (Harlow and Halpert, 1998; Domanski et al., 2001), indicating that CYP3A4 substrate and effector-binding sites are separate, but closely linked, and the residues involved in the binding of either substrate and/or effector depend on the molecule present.

The clinical significance of an observed in vitro heteroactivation of CYP3A4 is still uncertain, because to date few confirmations in vivo have been reported. A decrease in diclofenac steady-state plasma concentrations, observed upon the coadministration of quinidine in rhesus monkeys, is consistent with an in vitro activation interaction

This study was supported by GlaxoSmithKline, UK. Part of this study was presented at the 6th ISSX Meeting, October 7–11, 2001, Munich, Germany and was published in abstract form in *Drug Metab Rev* **33 (Suppl 1):**179.

[1] Abbreviations used are: P450, cytochrome P450; QUI, quinidine; HAL, haloperidol; MDZ, midazolam; TST, testosterone; NIF, nifedipine; FEL, felodipine; SV, simvastatin; 6β-HTS; 6β-hydroxytestosterone; OX NIF, oxidized nifedipine; FEL PYR, felodipine and pyridine metabolite; CYP3A4/OR, coexpressed CYP3A4 and NADPH-cytochrome P450 reductase.

Address correspondence to: Dr. J. B. Houston, School of Pharmacy and Pharmaceutical Sciences, University of Manchester, Oxford Rd., Manchester, M13 9PL, UK. E-mail: brian.houston@man.ac.uk

TABLE 1

Incubation and assay conditions for the substrates investigated

CYP3A4 Substrate	Protein Concentration	Incubation Time	Substrate Concentration	Assay
	mg/ml	*min*	*μM*	
MDZ	1.0	2.5	2, 5, 10 (HAL), 50	Sapelcosil LC-ABZ, 5 μM, 15 cm × 4.6 mm; 65% 0.025 M ammonium acetate (pH 5):35% acetonitrile, flow 1.0 ml/min; HPLC/UV-240 nm; retention times: 4-OH MDZ, 7 min; 1′-OH MDZ, 8 min; MDZ, 12 min; LOQ = 0.025 nmol, interassay CV < 5%
FEL	1.0	10	10, 25, 50	Extraction by ethyl acetate; Spherisorb 5 ODS2, 15 cm × 4.6 mm; 0.2% TMED (*N*,*N*,*N*′,*N*′-tetramethylethylenediamine) in water, pH 7.0):methanol (30:70, v/v); flow 1.0 ml/min, HPLC/UV, 235 nm; retention times: FEL-PYR, 7 min; FEL, 9 min; UK-58,790, 12 min; LOQ = 0.05 nmol, interassay CV < 5%
NIF	0.5	15	10, 20, 50, 200	Lightning C_{18} (33 mm × 3 mm, 4 μm); 61% acetonitrile:39% ammonium acetate (10 mM, pH 8); flow 0.7 ml/min; MS:positive ion MRM with Turbo ionspray interface (480°C); transitions: 345 → 284 (OX NIF); 480 → 315 (nicardipine, internal standard); LOQ = 0.0125 nmol, interassay CV < 5%
TST	0.5	15	25, 50, 100, 200, 500 (HAL)	Waters C_{18} Novapak (150 × 3.9 mm); 50% methanol:50% distilled water; flow 1.0 ml/min, HPLC/UV, 245 nm; retention times: 6β-HTS, 5 min; TST, 26 min; LOQ, 0.0125 nmol, interassay CV < 5%
SV	0.5	10	5, 10, 25, 50	ACE 5 C_{18} (10 cm × 4.6 mm); 85% 50 mM ammonium acetate:15% acetonitrile, gradient column temperature: 40°C, flow 1.0 ml/min; MS, Micromass LCT (time of flight mass spectrometer), positive ion full scan MS; LOQ = 0.01 nmol, interassay CV < 5%

(Tang et al., 1999; Ngui et al., 2000). Quinidine also shows the ability to stimulate meloxicam metabolism by CYP3A4 and increases the contribution of CYP3A4 over CYP2C9 to the overall metabolism by heteroactivation (Ludwig et al., 1999).

To explore these confounding factors of CYP3A4 drug-drug interactions we have selected quinidine (QUI) and haloperidol (HAL) as modifiers. Selection of QUI, a well known inhibitor of CYP2D6, was based on previous reports suggesting differential effects on various CYP3A4 substrates, ranging from inhibition (von Moltke et al., 1994; Kenworthy et al., 1999) to activation (Ludwig et al., 1999; Tang et al., 1999, Sai et al., 2000; Ngui et al., 2001). Similarly, the effects of HAL on various subclasses of CYP3A4 substrates (Kenworthy et al., 1999) were found to be inconsistent. Midazolam (MDZ), testosterone (TST), nifedipine (NIF), felodipine (FEL), and simvastatin (SV) were selected as representatives of a range of CYP3A4 substrates. The choice of TST, MDZ, and NIF was based on their in vitro kinetic properties, which include homotropic cooperativity, hyperbolic kinetics, and substrate inhibition, respectively. FEL was included to provide a comparison with NIF, based on the similarities in their metabolic pathways and the high correlation reported for their in vivo clearance (Soons et al., 1993). Selection of SV was based on its widespread clinical use and the significance of its drug-drug interactions.

To describe the experimental data, multisite kinetic models and the corresponding equations that assume the existence of either two or three distinct binding domains within the active site of CYP3A4 have been derived, based on a steady-state, rapid equilibrium approach (Segel, 1975). The substrate and effector kinetic properties, and the alterations in their binding affinities and catalytic efficiency when simultaneously present at the active site, are characterized by interaction factors. Based on the findings with HAL and QUI, certain criteria for a generic two-site model for drug-drug interactions involving CYP3A4 are defined.

Materials and Methods

Chemicals. TST, 6β-hydroxytestosterone (6β-HTS), NIF, QUI, MDZ, HAL, NADP, and isocitric dehydrogenase were purchased from Sigma Chemical (Poole, Dorset, UK). Oxidized NIF (OX NIF), (3*S*)-3-OH QUI, and MDZ metabolites were obtained from Ultrafine Chemicals (Manchester, UK). FEL and pyridine metabolite (FEL PYR) were gifts from Astra (Hässle, Mölndal, Sweden). SV was obtained from Merck (Darmstadt, Germany) and UK-58,790 was from GlaxoSmithKline (Frythe, UK). All other reagents and solvents were of high analytical grade. Microsomes from human B-lymphoblastoid cells with coexpressed CYP3A4 and NADPH-cytochrome P450 reductase (CYP3A4/OR) were obtained from Gentest (Woburn, MA).

Incubation Conditions. Interaction studies were performed at incubation times and protein concentrations within the linear range for the each substrate. Microsomes from cells containing recombinant human CYP3A4/OR were suspended in 0.1 M phosphate buffer, pH 7.4. The final incubation volume was 0.2 ml, containing 47 to 111 pmol of P450/ml. Samples were preincubated for 5 min in a shaking water bath at 37°C, and each reaction was initiated with an NADPH-regenerating system (1 mM $NADP^+$, 7.5 mM isocitric acid, 15 mM magnesium chloride, and 0.2 units of isocitric dehydrogenase). The substrates (concentrations defined below) were added to each incubation in either methanol or phosphate buffer, depending on the solubility. Neither of the substrates showed significant microsomal binding (<10%). The final concentration of methanol in incubation media was ≤0.5% (v/v). The range of HAL and QUI concentrations applied was from 0.5 to 100 μM in most studies. The reaction was terminated by 0.1 ml of ice-cold methanol. Samples were then centrifuged at 13,400*g* for 5 min and analyzed by high-performance liquid chromatography/ultraviolet or high-performance liquid chromatography with tandem mass spectrometry (Table 1).

Data Analysis. The kinetic parameters were calculated from untransformed data by nonlinear least-squares regression using GraFit 4 (Erithacus Software, Horley, Surrey, UK). In the case of FEL, MDZ, and SV, the Michaelis-Menten equation with the weighting factor of 1/y was used to analyze the data. Analysis of NIF kinetic data was carried out assuming single site Michaelis-Menten kinetics with substrate inhibition (Houston and Kenworthy, 2000). In the case of TST, kinetic parameters V_{max}, S_{50}, and Hill coefficient (n) were calculated from untransformed data using Hill equation. CL_{max} was calculated in case of TST as an alternative to CL_{int} (due to autoactivation phenomenon), providing an estimate for the maximum clearance when the enzyme is fully activated before the saturation occurs (Houston and Kenworthy, 2000). The changes in kinetic parameters observed in the presence of various modifiers were significance tested using analysis of variance.

To obtain a more precise description of the molecular events at the active site and to substantiate the existence of multiple substrate-binding sites, data were further analyzed by various two- and three-site models. Initial steps to enable the selection of a multisite kinetic model involved consideration of the rate profiles in the presence of a modifier (IC_{50} plots) and the changes in the kinetic parameters for the substrate of interest. All these kinetic models assume rapid equilibrium, i.e., the rate of complex dissociation is much faster than the rate of product formation (Segel, 1975). Two substrate-binding sites were assumed to be identical, with no distinguishable difference between ES and SE conformation. Complete data sets (n = 16–24) in presence and absence of modifier were fitted to the rate equations for different multisite kinetic models using GraFit. Several models

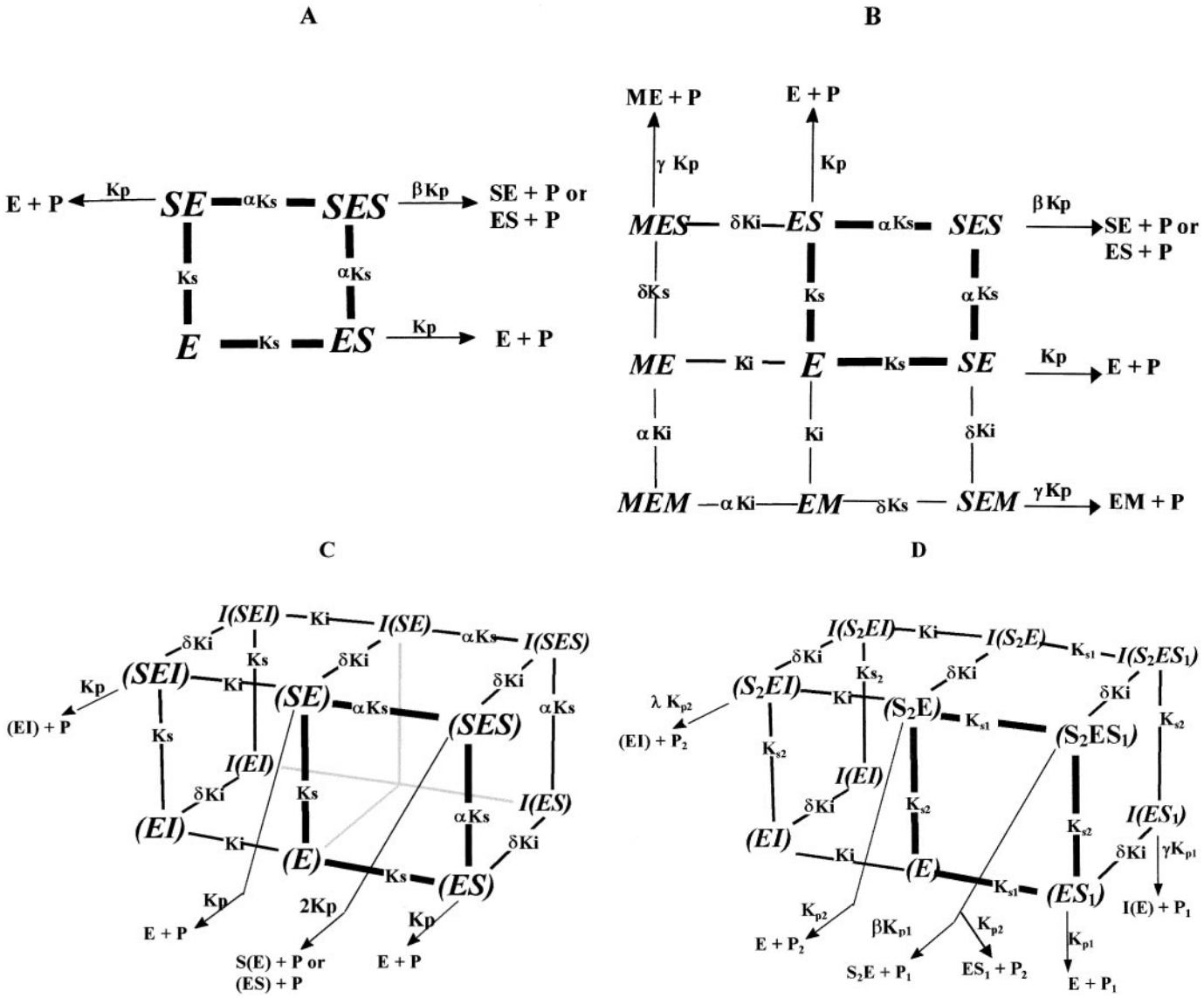

FIG. 1. *Multisite kinetic equilibria models.*

Kinetic model for an enzyme with two-substrate binding sites, the second substrate (S) molecule binds cooperatively K (A). Overall scheme for simultaneous metabolism of the S and modifier (M) in the active site upon binding to two sites (B). Three-site kinetic model for an enzyme where S binds cooperatively in the presence or absence of I at a distinct site (C). Three-site kinetic model with two distinct substrate-binding sites and pathway-differential effect of a modifier (D).

were tested for each data set, and the model with the least number of parameters and consistent with kinetic properties of both the substrate and modifier was selected. Goodness of fit was determined by comparison of statistical parameters (χ^2 and Akaike information criterion values) between the models and a reduction in the standard errors of the parameter estimates. Velocity curves for metabolite formation were simulated using the kinetic parameter estimates obtained from different multisite kinetic models.

Multisite Kinetic Equilibria Models. The kinetic models used were adopted from Segel (1975) and were based on steady-state and rapid equilibrium approach, allowing simultaneous fit of multiple sets of data to a single equation. The assumptions of this approach are outlined in this textbook.

Two-Site Models. The simplest model accommodating atypical kinetic properties when two molecules of the same substrate bind to the active site is presented in the Fig. 1A. Two binding sites are identical, because no orientation differences in binding of S to E were defined. Alterations in either binding affinity or catalytic efficiency upon binding of a second substrate molecule to a vacant site can describe data both from substrates showing positive cooperativity and substrate inhibition. The interaction of the substrate molecules is quantified by the velocity equation shown below:

$$\frac{v}{V_{max}} = \frac{\frac{[S]}{K_s} + \frac{\beta[S]^2}{\alpha K_s^2}}{1 + \frac{2[S]}{K_s} + \frac{[S]^2}{\alpha K_s^2}} \quad (1)$$

Autoactivation might be a result of either increased binding affinity for a second substrate molecule (K_s changes by the factor $\alpha < 1$), or changes in the effective catalytic rate constant (K_p) by the factor β in the two-substrate-bound complex ($\beta > 1$). Changes in α or β in the opposite direction can yield negative cooperativity ($\alpha > 1$, resulting in biphasic kinetic profile, $\beta < 1$, resulting in substrate inhibition) (Houston and Kenworthy, 2000).

Inhibition profiles obtained for NIF, FEL, SV, and MDZ were rationalized applying a range of kinetic models with two-substrate-binding sites, where modifier competes at both substrate-binding sites. These kinetic models describe various effects on CYP3A4, i.e., activation of the substrate metabolism and different types of inhibition, including mixed, partial, and competitive

inhibition for substrates with hyperbolic or substrate inhibition kinetic properties. The generic scheme for the two-site models is presented in Fig. 1B. Due to the fast release of products each substrate was considered independently, i.e., the metabolism of only one substrate was considered at a time. The alterations in binding affinity and product formation upon the binding of an effector molecule were taken into consideration by incorporating certain interaction factors (α and β, respectively).

There is the possibility that the enzyme-product complex reduces the enzyme availability for the S interaction, causing a decreased rate of the reaction (Narasimhulu et al., 1998). However, to keep the data analysis and modeling relatively simple, enzyme-product complexes were not included in the total sum of the product-forming complexes in the model derivation.

Inhibition/Activation of a Substrate with Hyperbolic Kinetics. Equation 2 is applied for the substrates showing hyperbolic type of kinetic properties (e.g., FEL). No interaction is observed between the substrate molecules (autoactivation); therefore, the kinetic model is simplified eliminating the interaction factor α. This two-site model can accommodate cases of partial inhibition and changes to K_s and V_{max} when the formation of a complex containing two different substrate molecules is more/less favorable, depending on the δ value. Interaction factor δ describes the changes in the binding affinities of the substrate and the modifier in the presence of each other. The equivalence of two-substrate-binding sites is assumed; therefore, β describing product formation from SES complex is 2, as V_{max} is equivalent to $2K_p[E]_t$, where $[E]_t$ is the total enzyme concentration. Alterations in the product formation in the presence of a modifier molecule are defined by the interaction factor $\gamma < 1$ for inhibition and $\gamma > 1$ for activation.

$$\frac{v}{V_{max}} = \frac{\frac{[S]}{K_s} + \frac{[S]^2}{K_s^2} + \frac{\gamma[S][I]}{\delta K_s K_1}}{1 + \frac{2[S]}{K_s} + \frac{[S]^2}{K_s^2} + \frac{2[S][I]}{\delta K_s K_1} + \frac{2[I]}{K_i} + \frac{[I]^2}{K_i^2}} \quad (2)$$

An identical model can be applied for activation; the only difference is the substitution of the inhibition terms (I and K_i) with the ones for activation (A and K_a).

Inhibition of a Substrate Showing Substrate Inhibition Kinetic Properties. Recent studies have indicated the utility of the kinetic models with two substrate-binding sites for the cases of substrate inhibition kinetics (Houston and Kenworthy, 2000; Lin et al., 2001; Schrag and Wienkers, 2001). The two-site model applied herein incorporates sequential binding of substrate molecules, i.e., the substrate inhibition site cannot be occupied until the active site is filled. The second site may be independent from the active site. Because the enzyme has only one catalytically active site, V_{max} is equivalent to K_p[E]t, where [E]t is the total enzyme concentration. The presence of the effector molecule may increase the complexity of the model, depending on the effector binding affinities and its effects on catalytic activities associated with the substrate-binding sites. Binding of a second substrate or inhibitor molecule causes a reduction in product formation, characterized by the interaction factor β ($0 < \beta < 1$) (eq. 3), because SES/IES/SEI are less productive.

$$\frac{v}{V_{max}} = \frac{\frac{[S]}{K_s} + \frac{\beta[S]^2}{K_s^2} + \frac{\gamma[S][I]}{\delta K_s K_i}}{1 + \frac{[S]}{K_s} + \frac{[S]^2}{K_s^2} + \frac{2[S][I]}{\delta K_s K_i} + \frac{2[I]}{K_i} + \frac{[I]^2}{K_i^2}} \quad (3)$$

Three-Site Models. These are more complex kinetic models where both substrate and effector bind to two sites, and one site is unique to either molecule (Kenworthy et al., 2001). The principal characteristics of three-site models is the existence of a distinct effector binding site, with the possibility of conformational changes upon the binding of the effector molecule, based on the model suggested by Ueng et al. (1997).

Heterotropic Inhibition of a Substrate Showing Sigmoidal Kinetics. Equation 4 is derived for the cases where a substrate binds cooperatively in the presence or absence of the inhibitor. This kinetic model was previously described for the effects of diazepam on TST (Kenworthy et al., 2001) and was applied here for QUI-TST interaction study. Similar to two-site models, the catalytic sites are assumed to be equivalent, therefore β would equal 2 in the corresponding equation and cancels out because V_{max} is equal to $2K_p[E]_t$, where $[E]_t$ is the total enzyme concentration. The interaction between two substrate molecules, and the sigmoidal properties of the substrate, are unaffected by increasing inhibitor concentration, suggesting that the inhibitor acts at a distinct effector site. Inhibition is not consistent with a competitive type, as the modifier causes changes in V_{max}, rather than changes in the substrate-binding constant K_s.

$$\frac{v}{V_{max}} = \frac{\frac{[S]}{K_s} + \frac{[S]^2}{\alpha K_s^2}}{1 + \frac{2[S]}{K_s} + \frac{[S]^2}{\alpha K_s^2} + \frac{[I]}{K_i} + \frac{2[S][I]}{K_s K_i} + \frac{[S]^2[I]}{\alpha K_s^2 K_i}} \quad (4)$$

Partial Inhibition of a Substrate Showing Sigmoidal Kinetics. Equation 5 defines another type of three-site models with two catalytically active substrate-binding sites and a distinct effector site. Similar to previous three-site model, cooperativity in substrate binding is maintained in the presence of an inhibitor. Binding of an inhibitor molecule to the separate effector site causes an alteration in K_i by the factor δ (Fig. 1C). In the cases where δ is >1, the affinity of the second inhibitor molecule is decreased in the presence of the first, consistent with negative cooperative effect, causing the partial inhibition with the increasing inhibitor concentration. The concentration and contribution of I(SEI), I(SE), and I(SES) complexes (Fig. 1C) to $[E]_t$ at higher inhibitor concentration is increased, but these enzyme species are not productive.

$$\frac{v}{V_{max}} = \frac{\frac{2[S]}{K_s} + \frac{[S]^2}{\alpha K_s^2} + \frac{[I][S]}{K_i K_s}}{1 + \frac{2[S]}{K_s} + \frac{[S]^2}{\alpha K_s^2} + \frac{[I]}{K_i} + \frac{[I][S]}{K_i K_s} + \frac{2[I][S]}{\delta K_i K_s} + \frac{[I]^2}{\delta K_i^2} + \frac{[S]^2[I]}{\alpha \delta K_s^2 K_i} + \frac{[I]^2[S]}{\delta K_i^2 K_s}} \quad (5)$$

Modifier Concentration-Dependent and Pathway-Differential Effects. The three-site kinetic model approach, required to describe interactions for substrates with sigmoidal kinetic properties, can also be used to describe the phenomenon of activation at low concentrations of the modifier changing to inhibition at higher concentrations. Equation 6 is derived for the 1′-OH MDZ formation and represents the three-site model with two distinct substrate-binding sites; ES_1 is preferable for 1′-OH MDZ (defined by K_{s1} and K_{p1}) and S_2E for 4-OH MDZ formation (K_{s2} and K_{p2}), with no alterations in the binding affinity for a second substrate molecule (Fig. 1D). However, the two occupied sites interact, changing the rate of 1′-OH MDZ formation (K_{p1} from SES complex is modified by the interaction factor β), analogous to a substrate inhibition phenomenon. Binding of the effector molecule stimulates 1′-OH MDZ formation at low substrate concentrations, increasing the V_{max} of the reaction and the effective catalytic rate constant from I(ES) complex compared to ES by the interaction factor γ (>1). Binding of a modifier molecule in the presence of MDZ is characterized by alterations in the inhibition constant K_i by the factor δ. At higher S concentrations, the second substrate-binding site is also occupied, causing the more pronounced substrate inhibition of 1′-OH pathway. Quinidine competes with MDZ for the mutual binding site, causing the inhibition of 1′-OH MDZ formation (increased K_m). At the same time, binding of a QUI molecule to a distinct site to one for 1′-OH MDZ alters kinetic properties of the substrate site preferential for the 4-OH formation, stimulating the metabolite formation (eq. 7, where λ is the interaction factor for the 4-OH pathway, $\lambda K_{p2} > K_{p2}$). Pathway differential effects observed for QUI were similar to the differential effects of α-naphthoflavone on losartan metabolism, reported by Shou et al. (2001a).

$$\frac{v}{V_{max1}} = \frac{\frac{[S]}{K_{s1}} + \frac{\beta[S]^2}{K_{s1}^2} + \frac{\gamma[I][S]}{\delta K_i K_{s1}}}{1 + \frac{[S]}{K_{s1}} + \frac{[S]}{K_{s2}} + \frac{[S]^2}{K_{s1}K_{s2}} + \frac{[I]}{K_i} + \frac{[I][S]}{\delta K_i K_{s1}} + \frac{[I][S]}{\delta K_i K_{s2}} + \frac{[I]^2[S]}{\delta K_i^2 K_{s2}} + \frac{[I][S]^2}{\delta K_i K_{s1} K_{s2}}} \quad (6)$$

$$\frac{v}{V_{max2}} = \frac{\frac{[S]}{K_{s2}} + \frac{[S]^2}{K_{s2}^2} + \frac{\lambda[I][S]}{K_i K_{s2}}}{1 + \frac{[S]}{K_{s1}} + \frac{[S]}{K_{s2}} + \frac{[S]^2}{K_{s1}K_{s2}} + \frac{[I]}{K_i} + \frac{[I][S]}{\delta K_i K_{s1}} + \frac{[I][S]}{\delta K_i K_{s2}} + \frac{[I]^2[S]}{\delta K_i^2 K_{s2}} + \frac{[I][S]^2}{\delta K_i K_{s1} K_{s2}}} \quad (7)$$

TABLE 2

Kinetic parameters for various CYP3A4 substrates in human lymphoblast-expressed CYP3A4 (mean ± S.E.)

CYP3A4 Substrate	Michaelis-Menten/Hill Equation				Two-Site Model		
	K_m/S_{50}	V_{max}	CL_{int}/CL_{max}	K_s	V_{max}	α	β
	μM	*pmol/min/pmol P450*	*μl/min/pmol P450*	*μM*	*pmol/min/pmol P450*		
TST 6β-hydroxylation[a]	42.7 ± 0.8	16.5 ± 0.2	0.22	93.5 ± 4.8	16.5 ± 0.2	0.15 ± 0.02	
NIF oxidation[b]	20.9 ± 2.2	9.7 ± 0.7	0.46	33.4 ± 4.9	12.8 ± 1.5		0.36 ± 0.08
FEL oxidation	26.4 ± 2.4	5.94 ± 0.23	0.22				
SV 3′-hydroxylation	35.1 ± 3.4	13.4 ± 0.5[c]					
MDZ 1′-hydroxylation	3.5 ± 0.5	4.8 ± 0.2	1.37				

[a] Sigmoidal kinetics, Hill coefficient = 1.34 ± 0.02, CL_{max} calculated as defined by Houston and Kenworthy (2000).
[b] Substrate inhibition, *K*si = 306 ± 55 μM, CL_{int} calculated as V_{max}/K_m ratio.
[c] Arbitrary number due to the lack of metabolic standards.

Results

The kinetic properties of the five CYP3A4 substrates selected for study were determined in human recombinant CYP3A4 system with coexpressed NADPH-P450 oxidoreductase (Table 2). NIF and TST showed the characteristics of substrate inhibition and sigmoidal kinetics, respectively, whereas MDZ, FEL, and SV displayed the standard hyperbolic curve. Less than 10% of the substrate depletion was noted and secondary metabolism was minimal throughout the course of incubation. Khan et al. (2002) have reported that MDZ can act as a mechanism-based inhibitor of CYP3A4, but incubation times used for MDZ were short (2.5 min), and no indication of inactivation was observed. A range of substrate concentrations (at least ½ K_m − 2K_m) was used to evaluate the effect of HAL and QUI. Both modifiers show substrate-dependent effects on CYP3A4 activity, ranging from potent inhibition (NIF), weak inhibition (TST), minimal effect (HAL on SV) to activation (QUI on FEL/SV).

Interaction with Nifedipine. Almost complete inhibition of NIF metabolism in human recombinant CYP3A4 was achieved with either HAL or QUI, with similar inhibitory effects across the range of substrate concentrations used. HAL was a potent inhibitor of NIF metabolism (IC_{50} = 0.1 μM; Fig. 2A) at substrate concentrations of 10 to 50 μM. The IC_{50} values in the QUI-NIF interaction study were higher and increased slightly with the increasing NIF concentrations (14.8–26.5 μM) (Fig. 3A).

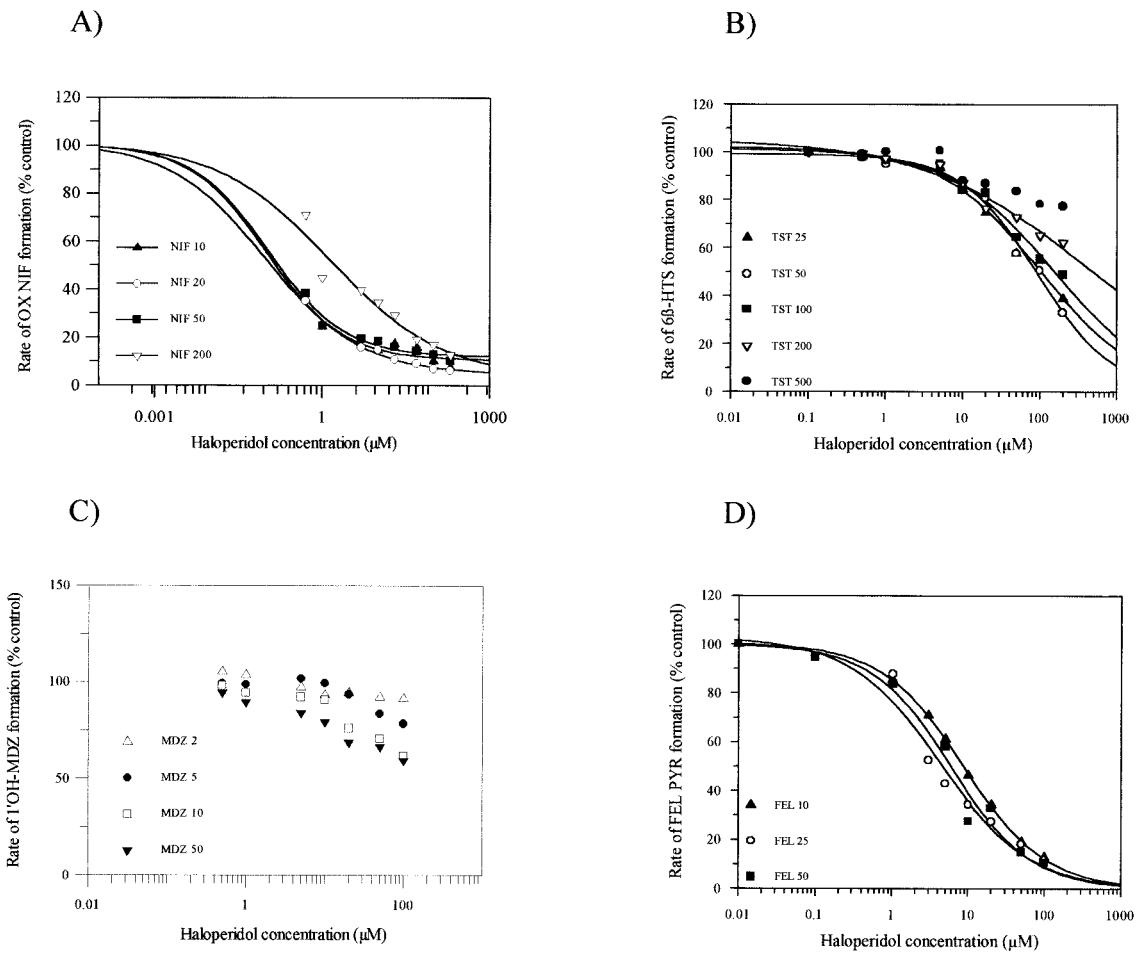

FIG. 2. *Effect of haloperidol on various CYP3A4 substrates in lymphoblast-expressed CYP3A4.*

NIF (10–200 μM) (A), TST (25–500 μM) (B), MDZ (2–50 μM) (C), and FEL (10–50 μM) (D).

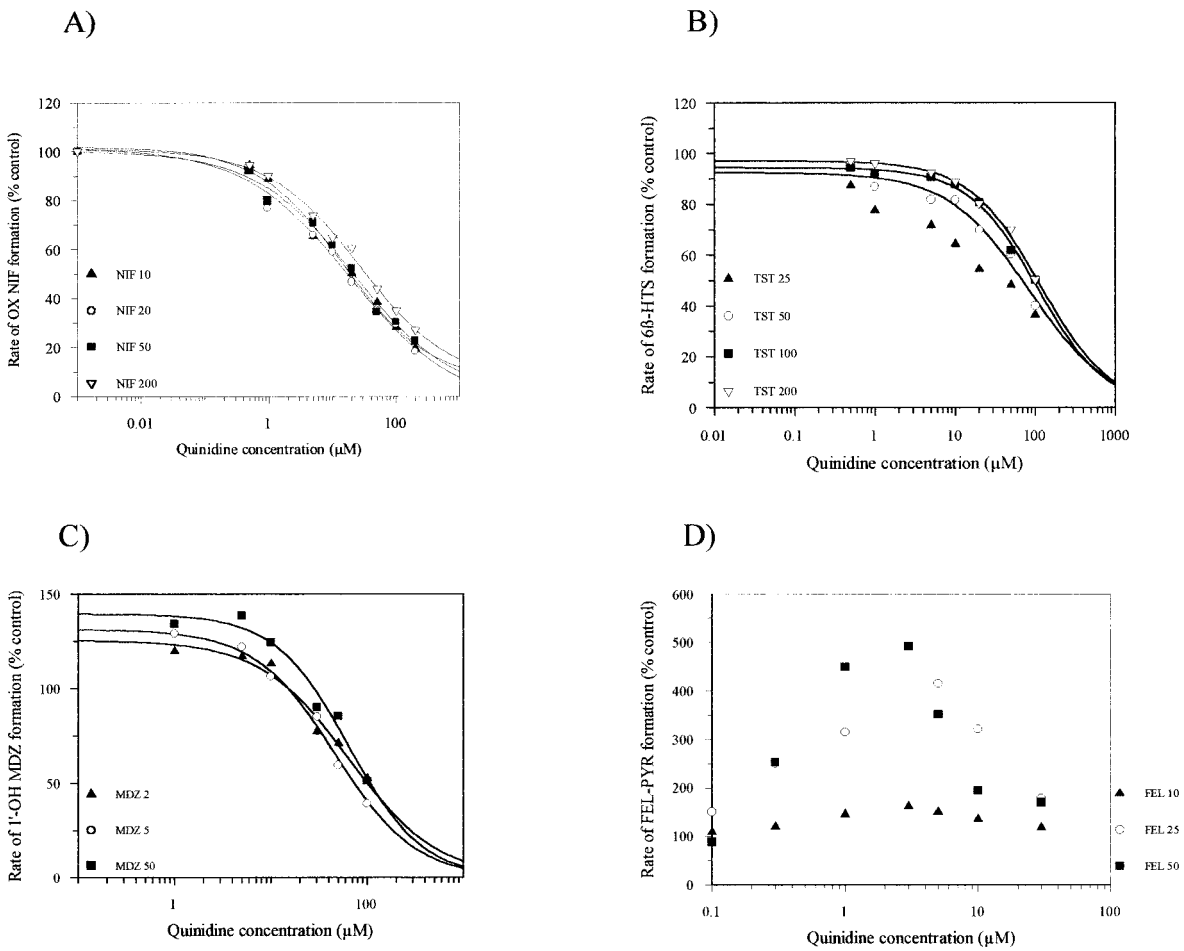

FIG. 3. *Effect of quinidine on various CYP3A4 substrates in lymphoblast-expressed CYP3A4.*
Substrate concentrations: NIF (10–200 μM) (A), TST (25–200 μM) (B), MDZ (2–50 μM) (C), and FEL (10–50 μM) (D).

Preliminary kinetic analysis performed by using the Michaelis-Menten equation both with or without substrate inhibition showed a 4-fold decrease in V_{max} values for OX NIF formation ($p < 0.05$) with the increasing concentrations of either HAL or QUI. In the presence of QUI, there was no statistically significant alteration in the K_m value, whereas a 3-fold increase was observed ($p < 0.05$) in the HAL-NIF study. At higher concentrations of both inhibitors, the substrate inhibition phenomenon observed for NIF is eliminated, resulting in the change of shape of the Eadie-Hofstee plot from the substrate inhibition "hook" to the linear relationship characteristic of Michaelis-Menten kinetics (Fig. 4A).

Two-site kinetic models were fitted to the data to rationalize the observed inhibition profiles. The kinetic parameters generated using the same two-site model (eq. 3) are presented in Tables 3 and 4, for the effects of HAL and QUI, respectively. The K_i values obtained for HAL and QUI were 0.25 and 5.3 μM, respectively. There was a substantial change in binding affinity of both modifiers in the presence of NIF, as defined by the interaction factor δ; the effect for HAL was 2-fold greater compared with QUI. Additionally, the higher inhibitory potency of HAL is seen in the lower value for γ, associated with the alterations in rate of product formation after binding of HAL to the active site. Substrate inhibition phenomena is eliminated at higher HAL/QUI concentrations as the more stable, but nonproductive S(EI) site dominates.

Interaction with Testosterone. The rate of TST 6β-hydroxylation in recombinant CYP3A4 was inhibited in the presence of increasing concentrations of either HAL (Fig. 2B) or QUI (Fig. 3B), but to a lesser extent than NIF. The shallow slope of IC_{50} plots (0.67–0.41) and the inability of HAL to fully inhibit TST metabolism, particularly at high substrate concentrations, were consistent with partial inhibition. In the QUI-TST interaction study, the inhibition profiles observed at higher substrate concentrations (50–200 μM) were similar, in contrast with the greater inhibition seen at the lowest TST concentration. The IC_{50} values for both modifiers progressively increased with increasing TST concentrations (34–114 and 98–386 μM for QUI and HAL, respectively) consistent with a competitive type of inhibition.

To select an appropriate CYP3A4 multisite kinetic model, the Hill equation was fitted to each individual set of data for HAL and QUI inhibition of 6β-HTS formation. Preliminary kinetic analysis showed a 2-fold increase in S_{50} values with the increasing HAL concentration (44.9–98.8 μM), whereas the V_{max} showed no statistically significant change. In QUI study, the V_{max} values decreased from 8.06 (control) to 4.11 pmol/min/pmolP450 (100 μM QUI) ($p < 0.005$), whereas no significant changes were observed in the S_{50}. Sigmoidicity of 6β-HTS formation remained over the range of concentrations of both HAL and QUI, with no significant changes in the Hill coefficient as indicated by the comparable extent of curvature in the Eadie-Hofstee plots (Fig. 4B). CL_{max} decreased 2-fold in the presence of increasing concentrations of HAL and QUI (Fig. 5B).

Tables 3 and 4 show the kinetic parameters generated from the fit to the three-site model, eq. 4 and 5, for QUI and HAL, respectively.

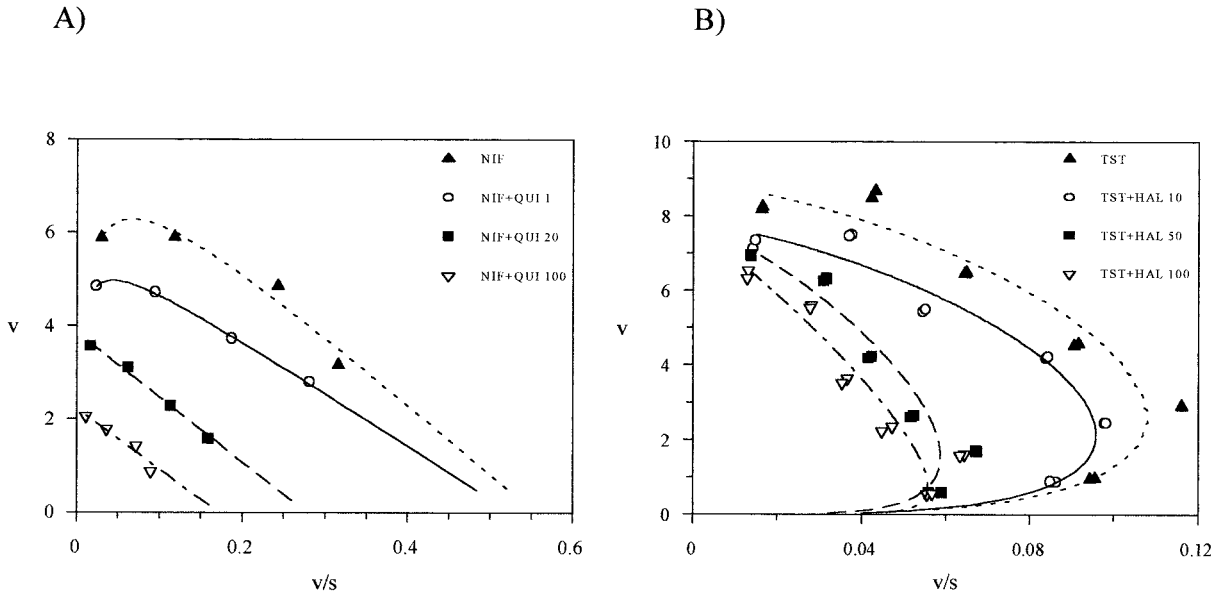

FIG. 4. *Eadie-Hofstee plots for OX NIF and 6β-HTS formation in the presence of QUI and HAL, respectively.*

NIF has substrate inhibition kinetic properties (A). TST has sigmoidal kinetics (B) the same as Fig. 2.

TABLE 3

Kinetic parameters for the in vitro interaction of haloperidol and various CYP3A4 substrates in human recombinant CYP3A4 generated by multisite kinetic model approach (mean ± S.E.)

CYP3A4 substrate	V_{max}	K_s	K_i	α	γ	δ
	pmol/min/pmol P450		*μM*			
NIF[a]	13.3 ± 1.3	34.9 ± 3.9	0.25 ± 0.13		0.32 ± 0.04	0.08 ± 0.03
FEL[b]	3.54 ± 0.31	40.9 ± 8.7	3.4 ± 0.9		0.95 ± 0.29	0.58 ± 0.19
TST[c]	8.41 ± 0.19	243 ± 17	34 ± 13	0.05 ± 0.02		8.2 ± 4.1

The kinetic parameters were determined using two-site model: [a]eq. 3, β (changes in K_p from SES) = γ and [b]; the kinetic parameters were determined using the eq. 2 $\beta = 2$ (substrate-binding sites are equivalent) three-site model: [c]eq. 5.

TABLE 4

Kinetic parameters for the in vitro interaction of quinidine and various CYP3A4 substrates in human recombinant CYP3A4 generated by multisite kinetic model approach (mean ± S.E.)

CYP3A4 Substrate	V_{max}	K_s	K_i	K_a	α	γ	δ
	pmol/min/pmol P450		*μM*				
NIF[a]	7.25 ± 1.24	16.7 ± 5.4	5.3 ± 2.4			0.81 ± 0.25	0.16 ± 0.03
TST[b]	8.27 ± 0.17	260 ± 35	99 ± 7		0.03 ± 0.01		
MDZ[c]	10.5 ± 2.1	14.5 ± 1.8	14.9 ± 2.7			1.8 ± 0.2	0.31 ± 0.11
FEL[d]	5.44 ± 0.18	52.8 ± 4.4		288 ± 75		9.8 ± 3.6	0.08 ± 0.04
SV[d]	11.9 ± 0.6[e]	80 ± 10		226 ± 65		2.6 ± 0.8	0.16 ± 0.05

The kinetic parameters were determined using two-site model: [a]eq. 3, β (SES) = 0.45 ± 0.11 and [d]eq. 2; the kinetic parameters were determined using the three-site model: [b]eq. 4 and [c]eq. 6 β (K_{p1} from S_2ES_1) = 0.29 ± 0.08, K_{s2} (4-OH MDZ site) = 22.6 ± 3.1 μM; [e]arbitrary number due to the lack of metabolite standards.

Simulated kinetic profiles for 6β-HTS formation at various QUI concentrations derived from those estimates are shown in Fig. 5A. The maintenance of cooperativity in TST binding in the presence of either inhibitor ($\alpha = 0.05$ and 0.03 for HAL and QUI study, respectively) indicates that the effector acts at a distinct site to the one responsible for TST metabolism. Both models assume two binding sites for the effector molecule, which is consistent with previously described effects of QUI and HAL on NIF. Partial inhibition of 6β-HTS formation in the presence of increasing HAL concentrations is consistent with a high δ value obtained. This alters the K_i value for HAL from 34 to 280 μM, illustrating a decreased binding affinity of the second HAL molecule (negative cooperativity) and reduced inhibitory effect at higher HAL concentrations. A reasonable fit to the simple partial inhibition model could not be obtained. The K_i value for QUI of 99 μM shows relatively weak inhibition of TST.

Interaction with Midazolam. HAL and QUI showed opposite effects on MDZ metabolism in human lymphoblast-expressed CYP3A4. HAL was a weak inhibitor and the highest extent of inhibition (around 40%) was observed at the highest MDZ concentration (Fig. 2C). In contrast, low concentrations of QUI activated MDZ 1′-hydroxylation (Fig. 3C), but at concentrations higher than 10 μM, inhibition of 1′-OH MDZ formation was observed. The extent of inhibition by QUI was approximately 50% of control values (5.28 pmol/min/pmolP450) at the highest MDZ concentration studied.

To obtain a general trend for the effects of QUI on MDZ metabolism, data for 1′-OH MDZ formation at various effector concentrations were first analyzed by the single-site approach. The V_{max} values for 1′-OH MDZ formation increased at lower QUI concentrations (3 μM) and decreased at higher (30 μM). At higher concentrations of the modifier a 5-fold increase in K_m value for the

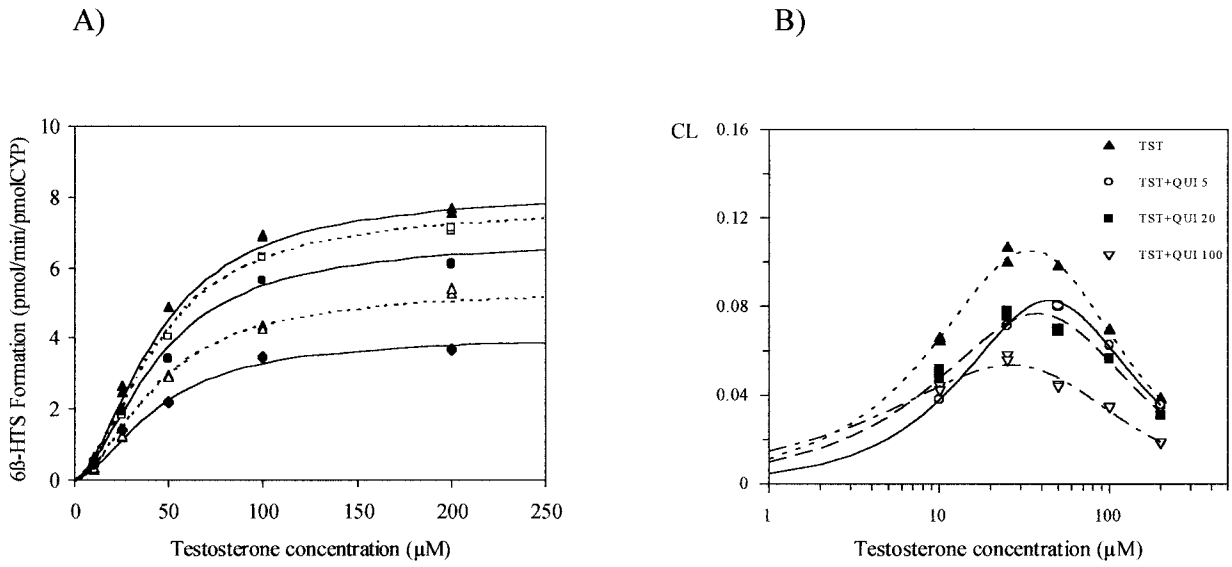

FIG. 5. *Effect of QUI on 6β-HTS formation.*

Kinetic profiles for 6β-HTS formation at QUI concentrations of 0 μM (▲), 5 μM (□), 20 μM (●), 50 μM (△), and 100 μM (◆); the solid and dashed lines represent the simultaneous fit to the eq. 4 at 10, 25, 50, 100, and 200 μM TST concentration (A) and the corresponding clearance plots (B).

same pathway was noted compared with the control. At the same time, QUI stimulated the formation of a minor metabolic product, 4-OH MDZ, up to 50% at 50 μM MDZ. The differential effects of QUI on MDZ 1′-OH and 4-OH metabolic pathways were particularly evident at higher concentrations of both the substrate (MDZ) and modifier (QUI) (Fig. 6).

Two binding-site models (applied for NIF) have the potential to describe the stimulation of substrate metabolism at low substrate concentrations, changing to inhibition with the increasing concentrations, but for these data an adequate fit could not be obtained. The use of a three-site kinetic model (eq. 6) was however successful. QUI competes with MDZ for the mutual site, activating the 1′-OH MDZ formation at low substrate concentration ($\gamma K_{p1} > K_{p1}$), changing to inhibition at higher concentrations of QUI (nonproductive complexes). The decreased product formation after the binding of the second substrate molecule ($\beta < 1$ from S_2ES_1 complex) is consistent with substrate inhibition (Fig. 7). Binding of QUI to the distinct effector site causes an allosteric effect on the substrate site preferential for 4-OH MDZ, stimulating this pathway.

Interaction with Felodipine. Contrary to expectation, the effects of HAL and QUI on FEL metabolism were not similar to the previously described NIF data. HAL was a potent inhibitor of FEL PYR formation (IC_{50} of ~5 μM), with similar inhibitory effects across the range of substrate concentrations used (Fig. 2D), whereas QUI stimulated FEL metabolism over a wide range of QUI concentrations, regardless of the substrate concentration investigated. At high concentrations of both FEL and QUI, the level of activation decreased, but no inhibition was evident (Fig. 3D).

To obtain a general trend for the effects of HAL and QUI on FEL, preliminary kinetic analysis was carried out assuming a single-site interaction. The simultaneous metabolism of FEL and HAL showed a decrease in V_{max} value for FEL formation from 4.42 to 1.39 pmol/min/pmolP450 (10 μM HAL) ($p < 0.01$) and an increase in the K_m value. The lack of any significant change in IC_{50} values was consistent with a mixed type of inhibition, observed also for NIF in the presence of HAL. Increased affinity of CYP3A4 for FEL over a range of QUI concentrations is manifested in a decrease in the K_m value and can be associated with the conformational changes in the substrate-binding site after binding of QUI molecule. This conformational change would allow FEL easier access to the active oxygen and results in increased catalytic activity (2-fold increase in the V_{max}).

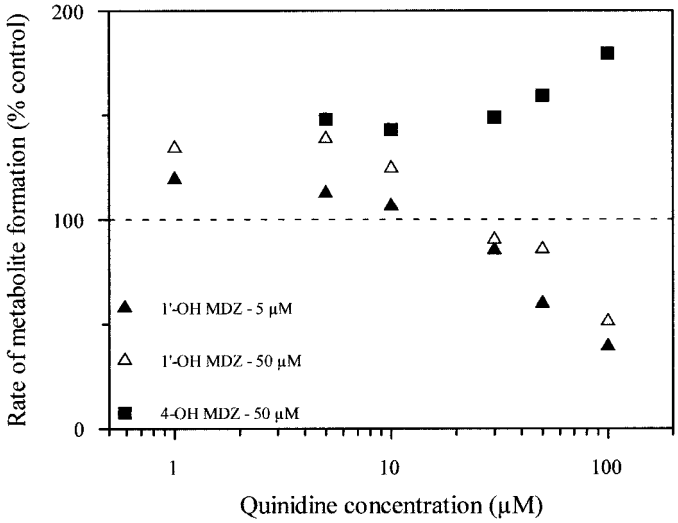

FIG. 6. *Differential effect of QUI on MDZ 1′- and 4-hydroxylation.*

Various two-site kinetic models were applied for further analysis of the contrasting effects of HAL and QUI on FEL CYP3A4-mediated metabolism. The kinetic parameter estimates for HAL, generated from a fit to eq. 2, are presented in Table 3. Potent inhibition ($K_i = 3.4$ μM) can be rationalized by the favorable formation of a complex containing both the substrate and modifier, as changes in γ are not pronounced. Estimates of the parameters generated from the fit to eq. 2 for the effects of QUI are shown in Table 4. The alteration in the binding affinity of substrate molecules is less pronounced in the presence of HAL ($\delta = 0.58$, K_s changes from 40.9 to 23.7 μM) compared with QUI ($\delta = 0.08$, K_s changes from 52.8 to 4.22 μM). Increased rate of FEL PYR formation from SEA/EAS complexes correlates well with the changes in the effective catalytic rate constant ($\gamma = 9.8$) for the QUI interaction.

Interaction with Simvastatin. The tendency for HAL and QUI to

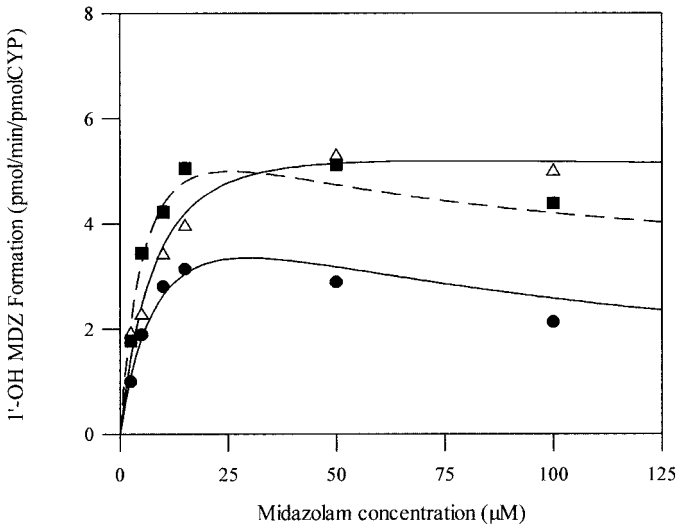

FIG. 7. *Effect of QUI on 1′-OH MDZ formation.*

Kinetic profiles for 1′-OH MDZ formation at QUI concentrations of 0 μM (△), 3 μM (■), and 30 μM (●); the solid and dashed lines represent the simultaneous fit to the eq. 6 at 2.5, 5, 10, 15, 50, and 100 μM MDZ concentration. Data points represent the mean of duplicate determinations.

produce opposite effects with certain CYP3A4 substrates was also seen with SV. Similar to the effect observed on MDZ 1′-hydroxylation, HAL was a weak inhibitor of the 3′-OH SV formation in human recombinant CYP3A4 (data not shown), and no further kinetic analysis was performed. Heteroactivation by QUI of the formation of 3′-OH SV, 6′-exomethylene SV, and 3′,5′-dihydrodiol SV occurred to a lesser extent compared with FEL and was mainly observed at low substrate concentrations. The K_a values obtained by two-site model (eq. 2) were similar (288 and 226 μM for FEL and SV, respectively), but the extent of changes in product formation and binding affinities (defined by γ and δ) were not as marked in SV study as with FEL (Table 4).

Discussion

The results presented here provide a systematic comparison of the interactions between five established CYP3A4 substrates and the modifiers HAL/QUI. Consistent with the substrate-dependent inhibition previously reported for CYP3A4 (Kenworthy et al., 1999; Wang et al., 2000), both modifiers were potent inhibitors of NIF metabolism and weak inhibitors of TST, while showing minimal effect (HAL on MDZ/SV) or activating the metabolism of other CYP3A4 substrates (QUI on FEL/SV).

Haloperidol K_i values varied >400-fold from 0.25 (NIF) to >100 μM (MDZ, SV), whereas activation and an 18-fold difference in QUI inhibitory potency was observed. A substrate-dependent effect was also observed in the rank order of potency, as HAL was more potent inhibitor of NIF, FEL, and TST metabolism, but MDZ 1′-hydroxylation was inhibited more effectively by QUI. In studies with NIF, FEL, and TST the rank order of inhibitory potency was in good agreement with the affinity of modifiers for CYP3A4 (50–78 μM for HAL; Pan et al., 1997) and 112 μM QUI (A. Galetin, unpublished data). Substrate-dependent effect of HAL was observed previously by Kenworthy et al. (1999), and it was suggested that HAL inhibits CYP3A4 at more than one site or that the inhibition site for HAL is not available with certain substrate-binding conformations. A range of HAL differential effects observed in the current study were all accommodated by kinetic models with two substrate-binding sites for HAL, indicating the flexibility of these models and their advantage over the previously proposed models with one substrate-binding site.

Quinidine has been shown to activate in vitro metabolism of fentanyl (Feierman and Lasker, 1996), meloxicam (Ludwig et al., 1999), phenanthrene (Sai et al., 2000), warfarin (Ngui et al., 2000), and both in vitro and in vivo metabolism of diclofenac (Tang et al., 1999). In all the studies, heteroactivation was a result of either changes in the binding affinities or changes to the effective catalytic rate constant in the presence of a modifier, or a combination of both effects. Ludwig et al. (1999) explained the increased affinity of CYP3A4 for meloxicam in the presence of QUI by a separate effector site. Binding of QUI to the effector site altered the character of a substrate-binding site, similar to an allosteric effect (Ueng et al., 1997). The observed activation of FEL and SV metabolism by QUI was best described by a kinetic model with two binding sites mutual for both the substrate and modifier (Fig. 1B). Heteroactivation occurred due to increased binding affinity of FEL in the presence of QUI ($\delta < 1$), together with increased product formation from the complex containing both QUI and FEL ($\gamma > 1$). Values for the interaction factors γ and δ were in the good agreement with the two-site models used to explain the heteroactivation of diclofenac (Tang et al., 1999) and warfarin (Ngui et al., 2001) by QUI. Stimulation of FEL metabolic pathway by QUI may also be explained by multiple conformer model approach suggested by Koley et al. (1995). Similar to NIF (Koley et al., 1997), FEL-QUI complex with CYP3A4 is more stable, but in this case also catalytically more active than the FEL complex, resulting in the stimulation of the reaction. In vitro heteroactivation of FEL and SV observed in the current study occurred at concentrations of QUI similar to its therapeutic plasma values (5 μM; Nielsen et al., 1999), indicating the possibility of an in vivo interaction, but the clinical significance remains to be determined. The K_i value of 5.3 μM obtained in the QUI-NIF study is also within the range of QUI plasma concentrations, indicating concern over possible drug-drug interaction in vivo.

Inhibition profiles for TST in the presence of QUI/HAL and the range of IC_{50} values obtained were in good agreement with Kenworthy et al. (1999) and Sai et al. (2000). However, the maintenance of cooperativity in TST binding in the presence of increasing HAL/QUI concentrations has not been noted previously due to insufficient number of substrate concentrations previously investigated. Three-site kinetic models with a distinct effector site adequately describe the observed inhibition profiles. Although three-site models are more complex, binding of HAL/QUI molecules to two sites is consistent with previously described kinetic models for the effects of HAL/QUI on NIF, FEL, and SV. Models assuming the existence of three binding sites, one for the substrate, one for the effector and one mutual for both, seem to be the models of choice for substrates showing cooperativity in their binding, as indicated for TST-diazepam interactions (Kenworthy et al., 2001).

Additionally, the differential effect of QUI on two MDZ metabolic pathways can be attributed to binding of QUI to a distinct effector site. Conformational changes in the substrate-site upon binding of QUI to a distinct effector domain and altered regioselectivity of MDZ metabolism are consistent with an allosteric model (Ueng et al., 1997). Thus, the modifying effects of QUI on CYP3A4 and QUI oxidation itself may not be associated with the same binding domains. This observation is consistent with site-directed mutagenesis studies and suggestions that behavior of α-naphthoflavone as a substrate or atypical activator/inhibitor of CYP3A4 was related to different locations within the CYP3A4 active site (Domanski et al., 2000).

Criteria for Selection of an Appropriate Multisite Kinetic Model in Prediction of Drug Interactions. The single-site Michae-

TABLE 5

Multisite kinetic model interaction factors to describe the various modifications of CYP3A4 activity

Effect on CYP3A4	Interaction Factor			Example
	α	γ*	δ	
Activation, S showing hyperbolic kinetics	1	>1	<1	QUI effect on FEL, SV QUI effect on diclofenac[a], warfarin[b]
Inhibition, S showing hyperbolic kinetics	1	<1	<1	HAL effect on FEL, QUI[c]
Inhibition, S showing substrate inhibition	1	<1 ($\beta < 1$, could = γ)	<1	QUI, HAL effect on NIF MDZ, FEL effect on NIF[c]
Partial inhibition, S showing hyperbolic kinetics	1	1	>1	NIF effect on FEL[c] TST-MDZ[c,e], TST-erythromycin[d], TST-Terfenadine[e]
Partial inhibition, S showing sigmoidal kinetics[g]	<1	1	>1	HAL effect on TST
Heterotropic activation, S showing sigmoidal kinetics[g]	<1	>1	$=\alpha$	TST effect on DZ[f]
Heterotropic inhibition, S showing sigmoidal kinetics[g]	<1	1	≤ 1	QUI effect on TST, DZ effect on TST[f]

* β (changes in K_p from SES) = 2 (equivalent binding sites).
[a] Ngui et al. (2000); [b]Ngui et al. (2001); [c]A. Galetin, unpublished data; [d]Wang et al., 1997; [e]Wang et al., 2000; [f]Kenworthy et al., 2000.
[g] Three-site model.

lis-Menten kinetic approach does not accommodate all kinetic features observed for CYP3A4 substrates, e.g., heteroactivation (Kenworthy et al., 2001), partial inhibition (Wang et al., 2000), substrate inhibition (Lin et al., 2001), and differential effects (Shou et al., 2001a). The finding that a number of CYP3A4 substrates do not conform to the expected competitive type of interaction indicates the existence of and interaction between several active sites. If restricted to using classical one-site models, the mixed kinetics would be most appropriate for the present findings. Some features of competitive inhibition occur in certain data sets, but not consistently (e.g., substrate-concentration dependence of IC_{50} values was observed in QUI-TST study, but the S_{50} values remained unchanged). The rate equations to describe the kinetic properties and interactions involving MDZ, NIF, FEL, TST, and SV with QUI and HAL accommodate at least two binding sites, and in some instances three. The large "active site" of CYP3A4 allows the simultaneous presence of multiple molecules and the exact binding conformations depend on the substrates involved, their relative concentration, and affinity for the enzyme.

The complexity of a kinetic interaction with a particular inhibitor/activator of CYP3A4 is dependent on the number of binding sites for both substrate and modifier, and their possible overlap. The positive cooperativity and substrate inhibition observed for TST and NIF, respectively, have been rationalized in terms of the binding of two substrate molecules to the active site (model A). This simple two-site model is extended to incorporate the presence of a modifier and the variety of inhibition types observed. The overall scheme presented in Fig. 1B can accommodate a range of effects observed for all the CYP3A4 substrates investigated, with the exception of TST. The two substrate-binding site model can be considered a generic kinetic model for drug-drug interaction studies for CYP3A4 substrates with hyperbolic or substrate inhibition kinetic properties. In contrast, models with three binding sites (Fig. 1C, distinct effector-binding domain) are more appropriate for the interactions of the substrates with cooperative binding to the active site (TST).

A summary of various effects accommodated by two-site kinetic models and the corresponding interaction factors associated with binding affinity/rate of product formation is presented in Table 5. The described interaction factors α, β, δ, and γ (Fig. 1B) can be included/excluded from the data modeling, depending on the substrate kinetics and the changes in the kinetic parameters in the presence of another substrate. The interaction factor α describes changes in binding affinity for a second molecule of the same substrate/modifier. Therefore, it can either be associated with substrate binding constant for substrates showing sigmoidal kinetics (TST), or with inhibitor binding constant in the cases of cooperative inhibition. The interaction factor δ describes a heterotropic effect and is required when formation of a complex with two different substrate molecules (MES) is favorable ($\delta < 1$). Either heteroactivation or inhibition may result, depending on the corresponding γ value (Table 5). In the cases where $\delta > 1$, the affinity of a second inhibitor molecule for a binding site is decreased compared with the first (TST inhibition by HAL), resulting in a partial inhibition with the increasing inhibitor concentration. The alterations in the K_p, associated with the interaction factors β (SES) and γ (MES) can be a result of substrate inhibition (NIF), heteroactivation (QUI-FEL), or inhibition (HAL-FEL). Depending on the effect, value of γ can range from <1 (inhibition) to >1 (activation) as illustrated in HAL-FEL and QUI-FEL interaction, respectively. In cases when the two occupied binding sites (SES) interact with no modification in the rate of product formation, β is 2, assuming the equivalence of the substrate binding sites.

Conclusion. The interaction data discussed above demonstrate that multisite enzyme kinetic models provide a good description of complex- and substrate-dependent CYP3A4 interactions. Application of the K_i values obtained in the prediction of inhibitory potency in vivo remains to be evaluated. Although the values of α, β, γ, and δ are substrate pair-dependent, certain trends can be observed based on kinetic properties of both the substrate and modifier. To accurately predict CYP3A4 inhibition potential, the evaluation of a possible inhibitor should be performed not only with substrates belonging to different subgroups, but also with substrates showing a range of kinetic properties (e.g., from hyperbolic to sigmoidal).

Acknowledgments. We thank Dr. Jackie Bloomer, Mike Nash, and Nigel Deeks (GlaxoSmithKline) for the analytical help in the project.

References

Domanski TL, HE Y-A, Harlow GR, and Halpert JR (2000) Dual role of human cytochrome P450 3A4 residue Phe-304 in substrate specificity and cooperativity. *J Pharmacol Exp Ther* **293:**585–591.

Domanski TL, HE Y-A, Khan KK, Roussel F, Wang Q, and Halpert JR (2001) Phenylalanine and tryptophan scanning mutagenesis of CYP3A4 substrate recognition site residues and effect on substrate oxidation and cooperativity. *Biochemistry* **40:**10150–10160.

Feierman DE and Lasker JM (1996) Metabolism of fentanyl, a synthetic opioid analgesic, by human liver microsomes. *Drug Metab Dispos* **24:**932–939.

Harlow GR and Halpert JR (1998) Analysis of human cytochrome P450 3A4 cooperativity: construction and characterization of a site-directed mutant that displays hyperbolic steroid hydroxylation kinetics. *Proc Natl Acad Sci USA* **95:**6636–6641.

Hosea NA, Miller GP, and Guengerich FP (2000) Elucidation of distinct ligand binding sites for cytochrome P450 3A4. *Biochemistry* **39:**5929–5939.

Houston JB and Kenworthy KE (2000) *In vitro-in vivo* scaling of CYP kinetic data not consistent with the classical Michaelis-Menten model. *Drug Metab Dispos* **28:**246–254.

Ito K, Iwatsubo T, Kanamitsu S, Ueda H, Suzuki H, and Sugiyama Y (1998) Prediction of pharmacokinetic alterations caused by drug-drug interactions: metabolic interaction in the liver. *Pharmacol Rev* **50:**387–411.

Kenworthy K, Bloomer JC, Clarke SE, and Houston JB (1999) CYP3A4 drug interactions: correlation of ten *in vitro* probe substrates. *Br J Clin Pharmacol* **48:**716–727.

Kenworthy KE, Clarke SE, Andrews J, and Houston JB (2001) Multi-site kinetic models for

CYP3A4: simultaneous activation and inhibition of diazepam and testosterone metabolism. *Drug Metab Dispos* **29:**1–8.
Khan KK, He YQ, Domanski TL, and Halpert JR (2002) Midazolam oxidation by cytochrome P450 3A4 and active-site mutants: an evaluation of multiple binding sites and of the metabolic pathway that leads to enzyme inactivation. *Mol Pharmacol* **61:**495–506.
Koley AP, Buters JTM, Robinson RC, Markowitz A, and Friedman FK (1995) CO binding kinetics of human cytochrome P450 3A4. *J Biol Chem* **270:**5014–5018.
Koley AP, Robinson RC, Markowitz A, and Friedman FK (1997) Drug-drug interactions: effect of quinidine on nifedipine binding to human cytochrome P450 3A4. *Biochem Pharmacol* **53:**455–460.
Korzekwa KR, Krishnamachary N, Shou M, Ogai A, Parise RA, Rettie AE, Gonzalez FJ, and Tracy TS (1998) Evaluation of atypical cytochrome P450 kinetics with two-substrate models: evidence that multiple substrates can simultaneously bind to cytochrome P450 active sites. *Biochemistry* **37:**4137–4147.
Lin Y, Lu P, Tang C, Mei Q, Sandig G, Rodrigues AD, Rushmore TH, and Shou M (2001) Substrate inhibition kinetics for cytochrome P450-catalyzed reactions. *Drug Metab Dispos* **29:**368–374.
Lu P, Lin Y, Rodrigues AD, Rushmore TH, Baillie TA, and Shou M (2001) Testosterone, 7-benzyloxyquinoline and 7-benzyloxy-4-trifluoromethyl-coumarin bind to different domains within the active site of cytochrome P450 3A4. *Drug Metab Dispos* **29:**1473–1479.
Ludwig E, Jochen S, Beschke K, and Ebner T (1999) Activation of human cytochrome P-450 3A4-catalyzed meloxicam 5′-methylhydroxylation by quinidine and hydroquinidine *in vitro*. *J Pharmacol Exp Ther* **290:**1–8.
Narasimhulu S, Havran LM, Axelsen PH, and Winkler JD (1998) Interactions of substrate and product with cytochrome P450: $P450_{2B4}$ versus $P450_{cam}$. *Arch Biochem Biophys* **353:**228–238.
Ngui JS, Chen Q, Shou M, Wang RW, Stearns RA, Baillie TA, and Tang W (2001) *In vitro* stimulation of warfarin metabolism by quinidine: increases in the formation of 4′- and 10-hydroxywarfarin. *Drug Met Dispos* **29:**877–886.
Ngui JS, Tang W, Stearns RA, Shou M, Miller RR, Zhang Y, Lin JH, and Baillie TA (2000) Cytochrome P450 3A4-mediated interaction of diclofenac and quinidine. *Drug Metab Dispos* **28:**1043–1050.
Nielsen TL, Rasmussen BB, Flinois J-P, Beaune P, and Brøsen K (1999) *In vitro* metabolism of quinidine: the (3*S*)-3-hydroxylation of quinidine is a specific marker reaction for cytochrome P-4503A4 activity in human liver microsomes. *J Pharmacol Exp Ther* **289:**31–37.
Pan LP, Weijnant P, De Vriendt C, Rosseel MT, and Belpaire FM (1997) Characterization of the cytochrome P450 isoenzymes involved in the *in vitro N*-dealkylation of haloperidol. *Br J Clin Pharmacol* **44:**557–564.
Rodrigues AD, Winchell GA, and Dobrinska MR (2001) Use of *in vitro* drug metabolism data to evaluate metabolic drug-drug interactions in man: the need for quantitative databases. *J Clin Pharmacol* **41:**1–6.
Sai Y, Dai R, Yang TJ, Krausz KW, Gonzalez FJ, Gelboin HV, and Shou M (2000) Assessment of specificity of eight chemical inhibitors using cDNA-expressed cytochromes P450. *Xenobiotica* **30:**327–343.
Schrag ML and Wienkers LC (2001) Triazolam substrate inhibition: evidence of competition for heme-bound reactive oxygen within the CYP3A4 active site. *Drug Metab Dispos* **29:**70–75.
Segel IH (1975*) Enzyme Kinetics: Behaviour and Analysis of Rapid Equilibrium and Steady State enzyme Systems.* Wiley & Sons, Inc., New York.
Shou M, Dai R, Cui D, Korzekwa KR, Baillie TA, and Rushmore TH (2001a) A kinetic model for the metabolic interaction of two substrates at the active site of cytochrome P450 3A4. *J Biol Chem* **276:**2256–2262.
Shou M, Grogan J, Mancewicz JA, Krausz KW, Gonzalez FJ, Gelboin HV, and Korzekwa KR (1994) Activation of CYP3A4: evidence for the simultaneous binding of two substrates in a cytochrome P450 active site. *Biochemistry* **33:**6450–6455.
Shou M, Lin Y, Lu P, Tang C, Mei Q, Cui D, Tang W, Ngui JS, Lin CC, Singh R, et al. (2001b) Enzyme kinetics of cytochrome P450-mediated reactions. *Curr Drug Metab* **2:**17–36.
Shou M, Mei Q, Ettore W Jr, Dai R, Baillie T, and Rushmore TH (1999) Sigmoidal kinetic model for two cooperative substrate-binding sites in a cytochrome P450 3A4 active site: an example of the metabolism of diazepam and its derivatives. *Biochem J* **340:**845–853.
Soons PA, Mulders TM, Uchida E, Schoemaker HC, Cohen AF, and Breimer DD (1993) Stereoselective pharmacokinetics of oral felodipine and nitrendipine in healthy subjects: correlation with nifedipine pharmacokinetics. *Eur J Clin Pharmacol* **44:**163–169.
Stresser DM, Blanchard AP, Turner SD, Erve JCL, Dandeneau AA, Miller VP, and Crespi CL (2000) Substrate-dependent modulation of CYP3A4 catalytic activity: analysis of 27 test compounds with four fluorometric substrates. *Drug Metab Dispos* **28:**1440–1448.
Tang W, Stearns RA, Kwei GY, Iliff SA, Miller RR, Egan MA, Yu NX, Dean DC, Kumar S, Shou M, et al. (1999) Interaction of diclofenac and quinidine in monkeys: stimulation of diclofenac metabolism. *J Pharmacol Exp Ther* **291:**1068–1074.
Tang W and Stearns RA (2001) Heterotropic cooperativity of cytochrome P450 3A4 and potential drug-drug interactions. *Curr Drug Metab* **2:**185–198.
Tucker GT, Houston JB, and Huang S-M (2001) Optimizing drug development: strategies to assess drug metabolism/transporter interaction potential: toward a consensus. *Clin Pharmacol Ther* **70:**103–114.
Ueng Y-F, Kuwabara T, Chun Y-J, and Guengerich FP (1997) Cooperativity in oxidations catalyzed by cytochrome P450 3A4. *Biochemistry* **36:**370–381.
von Moltke LL, Greenblat DJ, Cotreau-Bibbo MM, Harmatz JS, and Shader RI (1994) Inhibitors of alprazolam metabolism *in vitro*: effect of serotonin-reuptake-inhibitor antidepressants, ketoconazole and quinidine. *Br J Clin Pharmacol* **38:**23–31.
Wang RW, Newton DJ, Liu N, Atkins WM, and Lu AYH (2000) Human cytochrome P-450 3A4: *in vitro* drug-drug interaction patterns are substrate-dependent. *Drug Metab Dispos* **28:**360–366.
Wang RW, Newton DJ, Scheri TD, and Lu AYH (1997) Human Cytochrome P450 3A4-catalyzed testosterone 6β-hydroxylation and erythromycin *N*-demethylation. *Drug Metab Dispos* **25:**502–507.